Frost heave has been suggested as the driving mechanism for the development of patterned ground in permafrost terrains and alpine areas, where the seasonal motion of pore water and ice produce sorting and profiling of the ground surface in regular geometric patterns (*10*).

The physical basis for the persistence of unfrozen water below the normal melting point has been attributed to various mechanisms, including dipolar forces, density variations, and the pressure melting of ice (*11*). However, the National Research Council reports that there has been no consensus on the fundamental causes

> The limitations of all current models may be characterized collectively by simply stating that at present no model enjoys universal or general acceptance. . . . It is not certain that a deterministic formulation adequate for either the scientific or the engineering needs can be developed.

The present theory explains the ice phenomena as consequences of surface melting, and it predicts that similar effects should occur in other materials. However, although Eq. 7 is completely independent of the nature of the interactions, its universality rests on the assumption that the melt liquid is identical with the bulk. This is an approximation because a liquid is modified in the proximity of its boundaries, where it is more ordered (*12*). The range of the ordering depends on the nature of the liquid and the wall. Therefore the equation is strictly valid only in the limit $T \rightarrow T_0$, where d diverges. As T decreases, the layer thins and the proximity effect becomes more important; as a result, the pressure falls below the asymptotic relation in a nonuniversal manner.

REFERENCES AND NOTES

1. D. Nenow and A. Trayanov, *J. Cryst. Growth* **79**, 801 (1986).
2. A. A. Chernov, *Z. Phys. Chem. Liepzig* **269**, 941 (1988).
3. J. F. van der Veen, B. Pluis, D. van der Gon, in *Chemistry and Physics of Solid Surfaces* (Springer-Verlag, New York, 1988), vol. VII.
4. J. G. Dash, *Proceedings of the Solvay Congress on Surface Science*, F. W. De Wette, Ed. (Springer-Verlag, New York, 1988).
5. ———, *Contemp. Phys.* **30**, 89 (1989).
6. See, for example, L. D. Landau and E. M. Lifshitz, *Statistical Physics* (Pergamon, New York ed. 3, 1980), vol. 5, part 1, p. 73.
7. D. M. Anderson and N. R. Morgenstern, *Proc. Second Int. Conf. Permafrost* (National Academy of Sciences, Washington, DC, 1973), pp. 257–288.
8. Representative articles describing laboratory studies of frost heave are R. W. R. Koopmans and R. D. Miller, *Proc. Soil Sci. Soc. Am.* **30**, 680 (1966); F. J. Radd and D. H. Oertle, *Proc. Second Int. Conf. Permafrost* (National Academy of Sciences, Washington, DC, 1973), p. 377. M. Vignes and K. M. Dijkema, *J. Colloid Interf. Sci.* **49**, 165 (1974); M. B. G. M. Biermans, K. M. Dijkema, D. A. De Vries, *Nature* **264**, 166 (1976); S. W. Hopke, *Cold Regions Sci. Technol.* **3**, 111 (1980); M. Buil, J. Aiguirre-Puente, A. Soisson, *C. R. Acad. Sci. Paris* **293**, 653 (1981).
9. Committee on Permafrost of the Polar Research Board, *Ice Segregation and Frost Heaving* (National Academy Press, Washington, DC, 1984).
10. B. Hallet, S. P. Anderson, C. W. Stubbs, E. C. Gregory, *Proc. Fifth Int. Conf. Permafrost* (National Academy of Sciences, Washington, DC, 1988), vol. 1, p. 770.
11. D. H. Everett, *Trans. Faraday Soc.* **57**, 1541 (1961); M. Vignes-Adler, *J. Colloid Interf. Sci.* **60**, 162 (1977); R. D. Miller, *Cold Regions Sci. Technol.* **3**, 83 (1980); R. R. Gilpin, *J. Colloid Interf. Sci.* **68**, 235 (1980).
12. J. Q. Broughton, A. Bonissent, F. F. Abraham, *J. Chem. Phys.* **74**, 4029 (1981); D. Oxtoby and A. D. J. Haymet, *ibid.* **76**, 6262 (1982); J. N. Israelachvili and P. M. McGuiggan, *Science* **241**, 795 (1988); D. M. Zhu and J. G. Dash, *Phys. Rev. Lett.* **60**, 432 (1988); G. An and M. Schick, *Phys. Rev.* **B39**, 9722 (1989).

13. I thank G. An, M. B. Baker, M. P. Den Nijs, B. Hallet, and E. A. Stern for criticism and discussions, and R. Lipowsky for pointing out an error in an earlier version. This research was supported by NSF grant DMR 86-11466.

4 August 1989; accepted 13 October 1989

Air Ventilation by Recoil Aspiration in Polypterid Fishes

ELIZABETH L. BRAINERD, KAREL F. LIEM, CRISTIAN T. SAMPER

High-speed x-ray cine films synchronized with intra-pleuroperitoneal pressure measurements show that polypterid fishes aspiration breathe by the deformation and recoil of their bony-scaled integument. Paleozoic amphibians arose from ancient air-breathing fishes and retained piscine bony scales in V-shaped rows along the belly. These scales resemble those of modern polypterid fishes and may have contributed to inhalation by elastic recoil. The discovery that polypterid fishes breathe by recoil aspiration is the first evidence for aspiration breathing in any lower vertebrate. The use of recoil aspiration by polypterids shows that elastic storage in a stiff body wall can contribute to inhalation in animals with limited capacity for active aspiration.

MOST AIR-BREATHING FISHES, LACKing the diaphragm or movable ribs thought necessary for aspiration breathing, use a buccal pulse pump to fill their respiratory gas bladders (*1*). Aspiration has never been demonstrated in air-breathing fishes or amphibians, although its use has been suggested (*2*) and refuted (*3*) for the Amazonian fish *Arapaima*, and estivating lungfish may ventilate tiny amounts (<0.3 ml) of air by aspiration (*4*). We show that polypterid fishes ventilate their lungs by aspiration and that this is accomplished by the deformation and recoil of their bony-scaled integument. We call this novel ventilatory mechanism "recoil aspiration." The discovery that polypterid fishes breathe by recoil aspiration may affect our understanding both of early tetrapod breathing mechanics and of the role of elastic storage in ventilation.

The fundamental difference between pulse pump and aspiration ventilation is that in pulse pump systems air forces the lung to expand, whereas in aspiration systems air is sucked into the already expanding lung (*5*). In fishes using a buccal pulse pump, such as the bowfin, *Amia calva*, the mouth cavity expands to fill with air and compresses to pump air into the lung. The lung begins to fill only after the mouth is closed, and buccal cavity diameter decreases as lung diameter increases (Fig. 1).

The use of aspiration to fill the lungs in polypterid fishes is demonstrated by the pattern of buccal and lung diameter change shown in Fig. 1. Unlike *Amia* lung diameter, *Polypterus* lung diameter increases rapidly while the mouth is still open, and the buccal and lung diameters increase simultaneously. This pattern indicates that air is sucked into the lungs through the open mouth, rather than being forced in by a buccal pump. A mouthful of air is usually pumped onto the lungs at the end of inhalation, but this buccal air contributes less to the total ventilated volume than does the aspirated air (*6*) (Fig. 1, *Polypterus*, lung diameter increase after mouth is closed). Sometimes, however, the buccal air is simply expelled from the opercular openings at the end of the air-breath. X-ray cine films also show that polypterid fishes exhale through the opercular openings and inhale through the mouth: they do not, as others have suggested, breathe through the spiracles (*7*).

Aspiration breathing requires the generation of negative pressure in the body cavity surrounding the lungs. We have measured considerable negative pressures in the pleuroperitoneal cavities of two polypterid species, *Polypterus senegalus* and *Erpetoichthys calabaricus*. X-ray cine films synchronized with pressure measurements show that the most negative pleuroperitoneal pressure occurs at

Museum of Comparative Zoology, Harvard University, Cambridge, MA 01238.

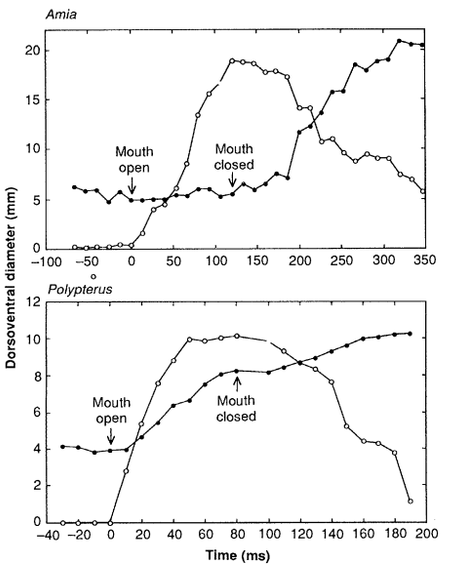

Fig. 1. Inspiration kinematics. Dorsoventral diameters of the buccal cavity and lung are shown during inspiration for the pulse pumper, *Amia calva*, and the aspiration breather, *Polypterus senegalus*. Solid circles represent lung diameter and open circles buccal diameter. Diameters were measured from x-ray cine films taken in lateral projection at a framing rate of 100 frames per second for *Polypterus* and 150 frames per second for *Amia*. Specimen size: *A. calva*, 27 cm; *P. senegalus*, 22 cm (length excluding caudal fin). Time zero corresponds to the end of expiration; only inspiration is shown. Note that in *Polypterus* the lungs begin to fill as soon as the mouth is opened and while the buccal cavity is still expanding.

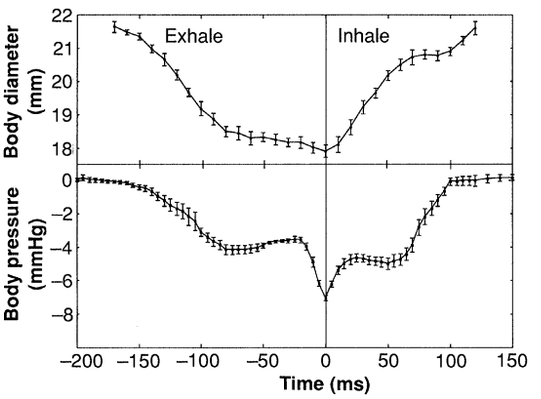

Fig. 2. Synchronized pleuroperitoneal cavity pressure and dorsoventral body diameter in *Polypterus*. The points represent mean values for six air-breaths from one 22-cm individual, and the bars represent ±1 standard error. As in Fig. 1, time zero corresponds to the beginning of mouth opening, which is also the time at which the most negative pleuroperitoneal pressures were measured and the body diameter reached its minimum. Experimental methods: dorsoventral body diameter was measured from lateral projection x-ray cine films (100 frames per second) at a position halfway between the pectoral girdle and the first dorsal spine. Pleuroperitoneal cavity pressures were read from the analog pressure trace at 5-ms intervals corresponding to each frame and half-frame. Pressures were recorded synchronously with the x-ray films. For pressure transducer implantation, fishes were anesthetized in a solution of tricane methanesulfonate. The pleuroperitoneal transducer was implanted through a small hole in the ventral integument and pushed through the hypaxial muscle layers to produce a tight seal around the lead wires. Pressures were measured with Millar Microtip SPR-249 pressure transducers and amplified with Millar TCB-500 transducer control units (*14*). Zero pressure corresponds to the ambient pressure at the level of the transducer.

the end of exhalation, just as the mouth begins to open for inhalation. In *P. senegalus*, this pressure has a mean magnitude of −5.7 ± 1.44 mmHg and a mean duration of 289 ± 41 ms (±1 standard deviation, n = 37 air-breaths from four individuals, size range 20 to 24 cm, length excluding caudal fin). In *E. calabaricus*, the mean magnitude is −4.5 ± 1.5 mmHg, and the mean duration is 318 ± 45 ms (n = 16 air-breaths from three individuals, size range 25 to 34 cm). In comparison, pleural cavity pressure during inhalation in resting humans is about −6 mmHg (*8*). Negative pressures of such magnitudes and durations are not seen in the body cavity of the pulse pumper *Amia*, which instead generates large positive body cavity pressures during air ventilation (*9*).

How can negative inspiratory pressures be generated without a diaphragm or movable ribs? Polypterid fishes are encased in a stiff scale jacket in which the scales are articulated by peg and socket joints into continuous scale rows (*10*). The timing of the production and resolution of negative pressure in relation to exhalation and inhalation indicates that these fishes exhale actively and then inhale by passive recoil of the scale jacket. If inhalation were actively produced, one would expect to see negative pressure only during inhalation. Instead, negative pressure is generated as the fish exhales and the scale jacket is deformed, and is resolved as air flows in to fill the lungs and the scale jacket returns to its original shape (Fig. 2). A sharp drop in pressure is seen just before the mouth begins to open for inhalation, and although we cannot rule out a direct, active component to this sudden dip, body diameter does show a small corresponding decrease that may account for the pressure drop. We conclude that the scale jacket is actively loaded upon exhalation and passively recoils to power inhalation (*11*) (Fig. 3). This ventilatory mechanism is not unknown among other vertebrates. Lampreys ventilate water by actively compressing their cartilaginous branchial basket, which then recoils to its original shape to draw in water (*12*).

The discovery of recoil aspiration in polypterids has important consequences for our understanding of the ventilation mechanics of early amphibians. Paleozoic amphibians retained ventral, bony scales from their air-breathing fish ancestors (*13*). These V-shaped scale rows are similar to the rhomboid scale body armor of polypterid fishes, and presumably both are derived from a distant, armored, gnathostome ancestor. The presence of recoil aspiration in polypterids suggests that the ventral scales of early amphibians may have contributed to aspiration ventilation in these forms.

The use of recoil aspiration by polypterid fishes demonstrates that a stiff body wall capable of storing energy can contribute to inhalation in animals with limited capacity for active aspiration. The discovery of this novel ventilatory mechanism suggests that it would be worthwhile to review the role of elastic storage during inhalation in a variety of vertebrates.

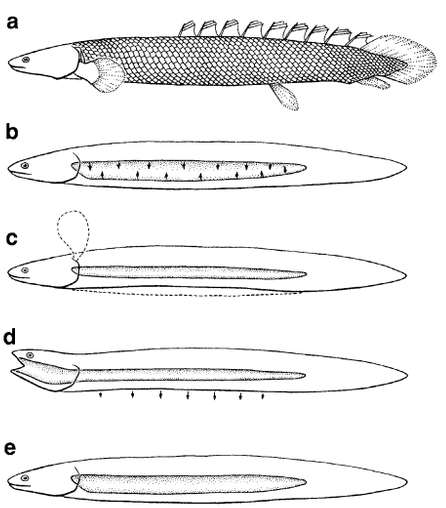

Fig. 3. A diagrammatic summary of the recoil aspiration model for polypterid ventilation. (**a**) A generalized polypterid showing the scale jacket. (**b**) During the initial phase of exhalation, the lung wall musculature contracts and pleuroperitoneal pressure begins to drop. (**c**) As the lungs are actively deflated, air is forced out through the opercular openings. The fluids and organs in the pleuroperitoneal cavity cannot change volume, and thus the ventral scale jacket is drawn inward to compensate for the change in volume produced by exhalation. This deformation stores elastic energy in the scale jacket, which results in negative pressure being generated in the pleuroperitoneal cavity. (**d**) During inhalation, air is sucked into the lungs as the scale jacket recoils to its original shape (**e**).

REFERENCES AND NOTES

1. D. J. Randall, W. W. Burggren, A. P. Farrell, M. S. Haswell, *The Evolution of Air-Breathing in Vertebrates* (Cambridge Univ. Press, Cambridge, 1981); K. F. Liem, *Am. Zool.* **28**, 793 (1988); B. McMahon, *J. Exp. Biol.* **51**, 407 (1969).

2. A. P. Farrell and D. J. Randall, *Can. J. Zool.* **56**, 939 (1978).
3. P. H. Greenwood and K. F. Liem, *J. Zool. London* **203**, 411 (1984).
4. J. P. Lomholt, K. Johansen, G. M. O. Maloiy, *Nature* **257**, 787 (1975).
5. C. Gans, *Forma Functio* **3**, 61 (1970).
6. Polypterid fishes have small heads in relation to their long bodies and lungs. The volume of air that buccal pumping can contribute to total ventilation is limited by the size of the buccal cavity. Volumes estimated from x-ray films combined with silicone casts of fresh specimens indicate that the maximum possible percentage of ventilation from buccal pumping is 24 ± 3% in *Erpetoichthys calabaricus* and 40 ± 5% in *Polypterus senegalus* (±1 standard deviation, $n = 3$ specimens of each species). With an elliptic cylinder as a model for the lungs, a rough calculation on the *Polypterus* air-breath in Fig. 1 shows that for an increase in the minor axis of the ellipse from 4 to 8 mm due to aspiration and from 8 to 10 mm due to buccal air, the contribution from buccal pumping is approximately 30%.
7. A. M. Abdel Magid, *Anim. Behav.* **14**, 530 (1966); *Nature* **215**, 1096 (1967); J. S. Budgett, *Proc. Zool. Soc. London* **15**, 323 (1901).
8. J. B. West, *Respiratory Physiology—The Essentials* (Williams & Wilkins, Baltimore, ed. 2, 1979).
9. E. L. Brainerd and K. F. Liem, unpublished data.
10. D. M. Pearson, *Zool. J. Linn. Soc.* **72**, 93 (1981).
11. Polypterid fishes do not have ribs surrounding the body cavity; their only ribs are dorsal ribs that do not extend ventrad below the lateral line (*10*). Since deformation during exhalation occurs in the belly, it seems unlikely that the ribs are involved in storing energy for recoil aspiration. The ribs may, however, be involved in stiffening the body laterally, thus allowing only dorsoventral deformation. Manipulation of unpreserved, dead specimens shows no tendency for recoil in the body wall after the integument has been removed. Passive recoil of the scale jacket was observed by compressing live and slightly anesthetized polypterids. Deeply anesthetized and dead specimens have no muscle tonus and thus become soft and flaccid. Recoil was observed in dead specimens, however, when pressure was applied to the sides of the specimen to hold the scale jacket in its natural alignment.
12. D. J. Randall, in *The Biology of Lampreys*, M. W. Hardisty and I. C. Potter, Eds. (Academic Press, London, 1972), vol. 2.
13. A. S. Romer, *Vertebrate Paleontology* (Univ. of Chicago Press, Chicago, 1966).
14. J. L. van Leeuwen and M. Muller, *Neth. J. Zool.* **33**, 425 (1983).
15. We thank F. A. Jenkins for his help and support throughout this work, E. Otten for discussions on energy storage, and C. Gans and D. Carrier for discussions on ventilation mechanics. Thanks to L. Meszoly for preparing Fig. 3 and to H. S. Kim and E. H. Wu for assistance with some of the experiments. Supported by an NSF grant to K.F.L.

11 July 1989; accepted 26 October 1989

The Anticodon Contains a Major Element of the Identity of Arginine Transfer RNAs

LaDonne H. Schulman and Heike Pelka

The contribution of the anticodon to the discrimination between cognate and noncognate tRNAs by *Escherichia coli* Arg-tRNA synthetase has been investigated by in vitro synthesis and aminoacylation of elongator methionine tRNA ($tRNA_m^{Met}$) mutants. Substitution of the Arg anticodon CCG for the Met anticodon CAU leads to a dramatic increase in Arg acceptance by $tRNA_m^{Met}$. A nucleotide (A20) previously identified by others in the dihydrouridine loop of $tRNA^{Arg}$s makes a smaller contribution to the conversion of $tRNA_m^{Met}$ identity from Met to Arg. The combined anticodon and dihydrouridine loop mutations yield a $tRNA_m^{Met}$ derivative that is aminoacylated with near-normal kinetics by the Arg-tRNA synthetase.

The molecular basis of the amino acid acceptor identity of tRNAs is still largely unknown, although progress has recently been made in determining structural features (identity elements) important for recognition of a number of *Escherichia coli* and yeast tRNAs by cognate aminoacyl-tRNA synthetases (*1–11*). Both biochemical and genetic experiments have indicated that the anticodon plays a role in defining the amino acid that will be attached to many tRNAs [reviewed in (*1*) and (*12*)]. However, the relative contribution of this sequence to tRNA identity has only been established in a few cases (*2, 11*).

Treatment of $tRNA_1^{Arg}$ (ICG) (the major Arg isoacceptor tRNA in *E. coli* having the anticodon ICG; I is inosine) with sodium bisulfite has been reported to result in loss of Arg acceptor activity by conversion of the anticodon base C35 to U35 (*13*). Chemical modification of G36 with ketoxal also inhibits its aminoacylation of $tRNA_1^{Arg}$ (ICG) (*14*), although modification of I34 with acetonitrile has no effect on recognition of the tRNA by Arg-tRNA synthetase (ArgRS) (*15*). Genetic experiments have shown that conversion of $tRNA_1^{Arg}$ (ICG) into an amber suppressor tRNA having the anticodon CUA results in partial loss of Arg activity and insertion of mostly Lys into protein at the site of amber codons (*1, 8*). These results indicate an important role for one or more anticodon bases in selection of tRNA substrates by ArgRS.

A composite structure of the nucleotides common to the primary sequences (*16*) of four *E. coli* $tRNA^{Arg}$s and bacteriophage T4 $tRNA^{Arg}$ is shown in Fig. 1. Comparison of this composite with the structure of the elongator $tRNA^{Met}$ ($tRNA_m^{Met}$) reveals that all of the bases conserved in $tRNA^{Arg}$s are present in $tRNA_m^{Met}$ except for the anticodon base C35 and A20 in the dihydrouridine loop. This suggests that one or both of these sites are important for discrimination against $tRNA_m^{Met}$ by *E. coli* ArgRS. McClain and Foss (*8*) have shown that conversion of A20 to U20 destroys the Arg acceptor identity of the amber suppressor tRNA, $tRNA_1^{Arg}$ (CUA), and that substitution of A20 + A59 into $tRNA^{Phe}$ (CUA) leads to insertion of mainly Arg by this tRNA at the site of amber codons in vivo. These elegant genetic experiments have clearly established the role of A20 as a component of Arg identity, but do not take into account the potential effect of C35 on the selection of these tRNA substrates by endogenous aminoacyl-tRNA synthetases or address the relative contribution of A20 and C35 to the efficiency of aminoacylation by ArgRS.

To study the structural basis for the discrimination against $tRNA_m^{Met}$ by ArgRS, we synthesized and assayed a series of $tRNA_m^{Met}$ derivatives. Wild-type and mutant tRNAs were prepared by in vitro transcription with T7 RNA polymerase as described before (*2*). Such transcripts contain none of the modified bases normally present in native tRNAs, but show near-normal amino acid acceptor activity with cognate aminoacyl-tRNA synthetases and are effectively discriminated against by noncognate enzymes (*2, 11, 17–19*). As expected, the transcript containing the sequence of wild-type $tRNA_m^{Met}$ (CAU) is efficiently aminoacylated with Met by MetRS, but is a very poor substrate for ArgRS (Table 1). The initial rate of Arg acceptance increases linearly with increasing $tRNA_m^{Met}$ (CAU) up to 40 μM, indicating that this concentration is much less than the Michaelis constant K_m for the tRNA. Under these conditions, accurate values for the kinetic parameters for Arg acceptance cannot be obtained, but the slope of the linear plot of initial rate versus $tRNA_m^{Met}$ (CAU) concentration gives V/K_m, where V is the maximal velocity. Comparison of V/K_m for the transcripts of $tRNA^{Arg}$ (CCG) and $tRNA_m^{Met}$ (CAU) shows that the relative specificity of ArgRS for its cognate tRNA is about seven orders of magnitude greater than that for the noncognate $tRNA^{Met}$. Substitution of A20 for U20 in wild-type $tRNA_m^{Met}$ produces a 1000-fold increase in V/K_m for Arg acceptance, whereas substitution of the Arg anticodon CCG for the Met anticodon CAU results in a 40,000-fold increase in specificity for ArgRS. A combination of these two changes, yielding

Department of Developmental Biology and Cancer, Albert Einstein College of Medicine, Bronx, NY 10461.